ISSN 0021-3640, JETP Letters, 2017, Vol. 106, No. 12, pp. 798–804. © Pleiades Publishing, Inc., 2017.
Original Russian Text © V.V. Val'kov, V.A. Mitskan, M.S. Shustin, 2017, published in Pis'ma v Zhurnal Eksperimental'noi i Teoreticheskoi Fiziki, 2017, Vol. 106, No. 12, pp. 762–768.

CONDENSED MATTER

Cascade of Quantum Transitions and Magnetocaloric Anomalies in an Open Nanowire

V. V. Val'kov*, V. A. Mitskan, and M. S. Shustin

Kirensky Institute of Physics, Federal Research Center Krasnoyarsk Scientific Center, Siberian Branch, Russian Academy of Sciences, Krasnoyarsk, 660036 Russia

**e-mail: vvv@iph.krasn.ru*

Received October 11, 2017; in final form, November 8, 2017

A sequence of magnetocaloric anomalies occurring with the change in a magnetic field H is predicted for an open nanowire with the Rashba spin–orbit coupling and the induced superconducting pairing potential. The nature of such anomalies is due to the cascade of quantum transitions related to the successive changes in the fermion parity of the nanowire ground state with the growth of the magnetic field. It is shown that the critical values H_c fall within the parameter range corresponding to the nontrivial values of the Z_2 topological invariant of the corresponding 1D band Hamiltonian characteristic of the D symmetry class. It is demonstrated that such features in the behavior of the open nanowire are retained even in the presence of Coulomb interactions.

DOI: 10.1134/S0021364017240134

1. INTRODUCTION

In recent years, the topological phases in superconducting systems have attracted considerable interest owing to the possibility of revealing there Majorana modes (MMs) [1, 2]. The promising objects for exhibiting MMs are semiconductor nanowires with the induced superconductivity in the presence of strong spin–orbit coupling and an applied uniform magnetic field [3]. The materials with a nonuniform external or exchange magnetic field belong to another class of such systems [4–6]. The Majorana modes can also manifest themselves in superfluid quantum liquids [7, 8] and in two-dimensional frustrated spin systems [9, 10].

The detection of MMs in open fermion systems is related to the finding of topologically nontrivial phases in the case of periodic boundary conditions. The most comprehensive classification of topological phases for noninteracting fermions was reported in [11, 12]. Later on, the methods for the classification of topological phases in 1D fermion systems with interactions were suggested in [13, 14]. The effect of onsite Coulomb correlations on the possible existence of a topological phase in the semiconductor nanowires with the spin–orbit coupling was also studied [15]. Moreover, the possibilities of finding a topological phase in the observed characteristics of nanowires were recently demonstrated [16, 17].

Tunnel spectroscopy and microscopy were employed to find in experiment the manifestations of MMs in the transport characteristics of semiconductor nanowires [18, 19] and in spin chains [20]. However, the MM identification based on the zero-bias conductance anomaly is still problematic, in particular, because of the existence of several mechanisms of anomalous conductivity [21, 22]. The interpretation of the tunnel conductivity data becomes more complicated also because the nanowires under study have the length $L \sim 100$ nm, which corresponds to the incoherent transport regime. It is usually accepted that the ballistic transport in such structures takes place at $L \sim 20$ nm, but the connection of such short nanowires to conducting leads currently encounters difficult technical problems.

It is important to note that the bulk–boundary correspondence in the conditions for existence of topologically nontrivial phases in the systems with periodic boundary conditions and for the existence of topologically protected MMs in the open systems comes into play only when the systems have sufficiently large spatial dimensions. Size effects in quantum nanowires, where MMs could manifest themselves, were studied in [23–28]. In particular, the oscillatory behavior of the energy splitting between the ground and first excited states as a function of the chain length and its parameter was reported in [26, 27]. Later on, for the model of a finite Kitaev chain [1], it was shown in [28] that the oscillations of the minimum excitation energy correspond to a sequence of quantum transitions (QTs) accompanied by a change in the fermionic parity of the ground state. Since the latter model describes a 1D ensemble of spinless fermions, the problems concerning the manifestations of QTs in the thermal and magnetic characteristics of the system have not been discussed.

In this work, we demonstrate that changes in the parameters of an open nanowire with a length $L \sim 10$ nm, the Rashba spin–orbit coupling, and the induced superconducting pairing potential also give rise to a cascade of QTs, which correspond to the changes both in the fermion parity and in the spin structure of the nanowire ground state. This results in the anomalous behavior of the magnetocaloric effect near quantum critical points. In this situation, the temperature variation rate near the QT point at the adiabatic variation of the magnetic field tends to infinity and has different signs on the left and on the right of the QT. This cascade of QTs takes place for a finite nanowire within a parameter range of the phase diagram where the state for an infinite nanowire is topologically nontrivial. We also demonstrate that relatively weak Coulomb interactions do not qualitatively change the aforementioned features.

2. FERMION PARITY OF THE GROUND STATE IN THE OPEN NANOWIRE

We consider a semiconductor nanowire located at the surface of the *s*-wave superconductor. In the applied magnetic field, the electron system of such nanowire can be described by the following Hamiltonian including the Rashba spin–orbit coupling:

$$\mathcal{H} = \sum_{n=1}^{N}\left[\Psi_n^+\left(-\mu\tau_z + h\sigma_z - \frac{\Delta}{2}\tau_+ - \frac{\Delta^*}{2}\tau_-\right)\Psi_n\right] + \sum_{n=1}^{N-1}\left[\Psi_n^+\left(-\frac{t}{2}\tau_z - \mathrm{i}\frac{\alpha}{2}\tau_z\sigma_y\right)\Psi_{n+1} + \text{H.c.}\right]. \quad (1)$$

Here, $\Psi_n^+ = \left(a_{n\uparrow}^+, a_{n\downarrow}^+, a_{n\downarrow}, -a_{n\uparrow}\right)$ is the standard Nambu notation, where $a_{n\sigma}$ ($a_{n\sigma}^+$) is the annihilation (creation) operator for an electron at the nth site having the spin projection σ on the quantization axis; μ is the chemical potential; t is the amplitude of electron hoppings between the nearest-neighbor sites; Δ is the amplitude of the *s*-wave superconducting pairing; and α is the Rashba spin–orbit coupling constant. The Pauli matrices σ_i and τ_i act in the spin and electron–hole spaces, respectively, and $\tau_\pm = (\tau_x \pm \mathrm{i}\tau_y)/2$.

It is convenient to rewrite Hamiltonian (1) in the Bogoliubov–de Gennes form

$$\mathcal{H} = \frac{1}{2}\mathbf{C}^+ H\mathbf{C}, \quad (2)$$

$$H = \begin{pmatrix} A_{\uparrow\uparrow} & A_{\uparrow\downarrow} & B_{\uparrow\uparrow} & B_{\uparrow\downarrow} \\ A_{\uparrow\downarrow}^+ & A_{\downarrow\downarrow} & -B_{\uparrow\downarrow}^T & B_{\downarrow\downarrow} \\ -B_{\uparrow\uparrow}^* & -B_{\uparrow\downarrow}^* & -A_{\uparrow\uparrow}^* & -A_{\uparrow\downarrow}^* \\ B_{\uparrow\downarrow}^+ & -B_{\downarrow\downarrow}^* & -A_{\uparrow\downarrow}^T & -A_{\downarrow\downarrow}^* \end{pmatrix}, \quad (3)$$

where $\mathbf{C}^+ = \left(\mathbf{a}_\uparrow^+, \mathbf{a}_\downarrow^+, \mathbf{a}_\uparrow^T, \mathbf{a}_\downarrow^T\right)$, and $\mathbf{a}_\sigma = (a_{1\sigma}, \ldots, a_{N\sigma})^T$. The matrices $\mathbf{A}_{\sigma,\sigma'}$, and $\mathbf{B}_{\sigma,\sigma'}$ have the following nonzero components ($A_{\sigma\sigma} = A_{\sigma\sigma}^+$, $B_{\sigma\sigma} = 0$):

$$\left(A_{\uparrow\downarrow}\right)_{n,n+1} = -\left(A_{\uparrow\downarrow}\right)_{n+1,n} = -\frac{\alpha}{2}, \quad \left(B_{\uparrow\downarrow}\right)_{n,n} = -\Delta^*, \quad \left(A_{\sigma\sigma}\right)_{n,n} = -\mu + \sigma h, \quad \left(A_{\sigma\sigma}\right)_{n,n+1} = -\frac{t}{2}. \quad (4)$$

The eigenvectors $\mathbf{Y}_m = \left(\mathbf{u}_{\uparrow m}, \mathbf{u}_{\downarrow m}, \mathbf{v}_{\uparrow m}^*, \mathbf{v}_{\downarrow m}^*\right)^T$ of the Bogoliubov–de Gennes Hamiltonian (3) describe the electron- and hole-like wavefunctions for the states with the excitation energy ε_m.

Hamiltonian (2) has the electron–hole symmetry, is characterized by the broken time-reversal invariance, and belongs to the D symmetry class. Its topological characteristics are classified according to the Z_2 invariant [12], which is expressed in terms of the fermion parity P of the ground state for sufficiently long closed chains [1].

To calculate the fermion parity, we write matrix (3) in the representation of Majorana operators

$$\gamma_{An\sigma} = a_{n\sigma} + a_{n\sigma}^+; \quad \gamma_{Bn\sigma} = \mathrm{i}(a_{n\sigma}^+ - a_{n\sigma}),$$

which are self-conjugated, $\gamma_{A(B)n\sigma} = \gamma_{A(B)n\sigma}^+$.

In the Majorana representation, the Bogoliubov–de Gennes Hamiltonian matrix $\tilde{H}$ is real and antisymmetric:

$$\tilde{H} = R^T H \Lambda R, \quad R = \begin{pmatrix} \hat{I} & -\mathrm{i}\hat{I} \\ \hat{I} & \mathrm{i}\hat{I} \end{pmatrix}, \quad \Lambda = \begin{pmatrix} \hat{0} & \hat{I} \\ \hat{I} & \hat{0} \end{pmatrix}, \quad (5)$$

where $\hat{I}$ is the $2N \times 2N$ identity matrix. Then, the fermion parity of the ground state of the chain can be calculated as the sign of the Pfaffian

$$P = \mathrm{sgn}\left(\mathrm{Pf}\left(\tilde{H}\right)\right) = \mathrm{sgn}\left(\det\left(W\right)\right). \quad (6)$$

Here, W is the real orthogonal matrix transforming $\tilde{H}$ to a block-diagonal form with nonzero diagonal blocks (2×2):

$$\begin{pmatrix} 0 & \varepsilon_m \\ -\varepsilon_m & 0 \end{pmatrix}.$$

At $P = 1$, the ground state of the chain is described by the superposition of states with an even number of fermions. The case of $P = -1$ corresponds to the ground state with the partial contributions involving odd numbers of fermions. For sufficiently long closed chains with even numbers of sites (their length far exceeds the characteristic spatial scales of the edge

states in the open chains[1]), the fermion parity is usually referred to as the Majorana number $\mathcal{M}$, and it is the Z_2 topological invariant [12].

3. OSCILLATIONS OF THE FERMION PARITY IN THE OPEN NANOWIRE

For the open nanowire, the calculated fermion parity allows us to construct the phase diagram shown in Fig. 1. The shaded areas correspond to $P = -1$. The boundaries of these areas are the curves corresponding to parameters for which the ground state is doubly degenerate and, hence, the minimum excitation energy vanishes.

Note that, for the closed infinitely long chain, the topologically nontrivial region (with $\mathcal{M} = -1$) is described by the inequalities

$$\sqrt{|\Delta|^2 + (\mu - |t|)^2} < |h| < \sqrt{|\Delta|^2 + (\mu + |t|)^2}.$$

In Fig. 1, the boundaries of this region are denoted by the dashed lines. The correspondence to an open chain with the finite number of sites N manifests itself in the location of all shaded areas within the topologically nontrivial parameter range. With the increase in N, the number of parity change lines grows, and in the limit $N \to \infty$, they form a quasicontinuum in the range of parameters with $\mathcal{M} = -1$.

Zero modes occurring at the lines of change of the fermion parity P are described by the wavefunctions localized near the chain edges. We can analyze the characteristics of these functions considering the behavior of the quasiparticle mode with the minimum nonnegative energy ε_0, described by the operator α_0:

$$\alpha_0 = \frac{1}{2}\sum_{n=1;\sigma}^{N}\left(w_{n\sigma,0}\gamma_{An\sigma} + z_{n\sigma,0}\gamma_{Bn\sigma}\right), \quad (7)$$

$$w_{n\sigma,0} = u^*_{n\sigma,0} + v_{n\sigma,0}, z_{n\sigma,0} = \mathrm{i}(u^*_{n\sigma,0} - v_{n\sigma,0}).$$

In the upper panel of Fig. 2, we illustrate the modification of $w = \sum_\sigma |w_{n\sigma,0}|^2$ as a function of the site number with the variation of the applied magnetic field h for the open chain consisting of 30 sites. The parameters of model (2) are the same as in Fig. 1, but the chemical potential is fixed, $\mu = 0.5|t|$. From Fig. 2, it follows that the amplitude of the wavefunctions for the edge modes appearing on the lines where the parity P changes has maximum values near the chain edges and is exponentially small in the middle of the chain. At the same time, there exists a weak hybridization of the wavefunctions to two bounded Majorana states, Γ_A and Γ_B, localized near different edges of the chain. The wavefunctions of these states are described by coefficients $w_{n\sigma,0}$ and $z_{n\sigma,0}$, respectively (see the lower panel in Fig. 2). With an increase in N, the degree of hybridization for the wavefunctions of bounded Majorana states decreases; this is well known from the available publications (see, e.g., [26, 27]).

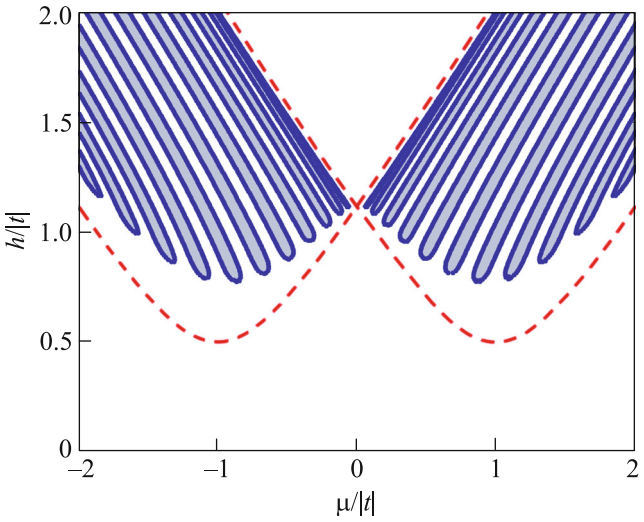

Fig. 1. (Color online) Phase diagram of the open nanowire ($N = 30$) with the induced superconducting pairing potential ($\Delta = 0.5|t|$) and the Rashba spin–orbit coupling ($\alpha = 0.8|t|$). The shaded areas correspond to such values of the model parameters for which the ground state includes the partial contributions corresponding to an odd number of fermions. The boundaries of these areas are the lines at points of which the Majorana mode appears. The dashed lines depict the boundaries of the range of existence for the topologically nontrivial phase in the long closed nanowire.

Let us emphasize that, for a short open chain, we have $\varepsilon_0 \cong 0$ only near the fermion parity change lines. Hence, the zeroth modes appearing on these lines are unstable with respect to random fluctuations of the parameters.[2] This is a fundamental difference between the short and long chains: for the latter, the minimum excitation energy can be infinitesimally close to zero (owing to exponentially small $\varepsilon_0 \sim \exp(-N)$) within a broad range of parameters corresponding to nontrivial values of the Z_2 invariant: $\mathcal{M} = -1$. However, it is important that the parametric lines on which we have zeroth modes for short open chains correspond to the region with $\mathcal{M} = -1$. Therefore, the identification of the fermion parity change lines using the thermal characteristics of a short open nanowire can indicate the parameter range where the topologically protected MMs can exist for the infinitely long open nanowire.

[1] We are grateful to the referee for these important remarks.

[2] We are grateful to the referee for these important remarks.

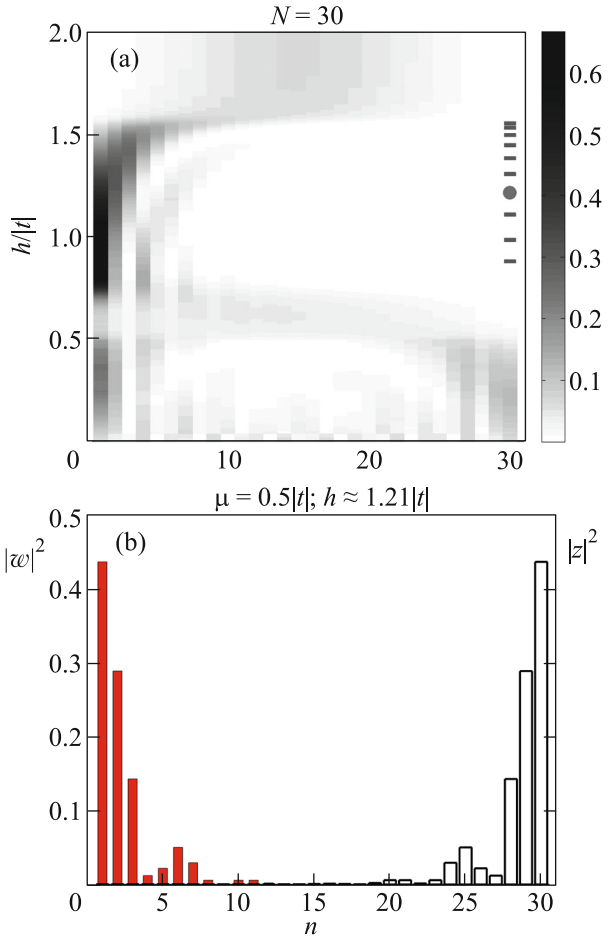

Fig. 2. (Color online) (a) $|w|^2 = \left|\sum_\sigma w_{n\sigma,0}\right|^2$ versus the magnetic field h and subscript n enumerating the sites. The correspondence between the values of $|w|^2$ and the colors on the map is given on the right side of the figure. The chemical potential is $\mu = 0.5|t|$ and the other parameters are the same as in Fig. 1. The behavior of $|z|^2 = \left|\sum_\sigma z_{n\sigma,0}\right|^2$ is similar to that of $|w|^2$ if we make the substitution $n \to N - n + 1$. The dashes and the point on the right side mark the h values at which the states with zero excitation energy occur. (b) Behavior of $|w|^2$ and $|z|^2$ at h corresponding to the point in panel (a).

4. MAGNETOCALORIC ANOMALIES AS SIGNATURES OF THE FERMION PARITY CHANGE LINES

At zero temperature, changes in the parameters characterizing a nanowire (both open and closed) lead to a sequence of quantum phase transitions accompanied by the changes in the fermion parity. At nonzero temperatures, QTs in magnetic systems can be identified by the analysis of the magnetocaloric effect (MCE) [11, 29], which manifests itself in the temperature change at the adiabatic variation of the applied magnetic field

$$\left(\frac{dT}{dh}\right)_{S,\mu} = -\frac{(\partial S/\partial h)_{T,\mu}}{(\partial S/\partial T)_{h,\mu}} = -T\frac{\left(\partial\langle S^z\rangle/\partial T\right)_{h,\mu}}{C(h,T)}, \quad (8)$$

$$\partial\langle S^z\rangle/\partial T = \frac{1}{2T^2}\sum_{m=1}^{2N} B_m \varepsilon_m f(\varepsilon_m)(1 - f(\varepsilon_m)), \quad (9)$$

$$C(h,T) = \frac{1}{T^2}\sum_{m=1}^{2N} \varepsilon_m^2 f(\varepsilon_m)(1 - f(\varepsilon_m)), \quad (10)$$

where

$$B_m = \sum_{n=1}^{N}\left(|u_{n\uparrow,m}|^2 - |u_{n\downarrow,m}|^2 + |v_{n\downarrow,m}|^2 - |v_{n\uparrow,m}|^2\right).$$

The analysis of Eqs. (8)–(10) demonstrates that, at low temperatures near zero-mode lines (where $\varepsilon_0 \to 0$), the magnitude of the MCE is of the order of $1/\varepsilon_0$ and diverges on the zero-mode lines. Moreover, this characteristic changes its sign upon passing the QT lines. The magnetic field dependence of the MCE for the chain consisting of 30 sites for the parameters corresponding to Fig. 2 is plotted in Fig. 3. The dashed lines depict the behavior of the MCE for the closed chain in the case $\mu = 0.5|t|$, where two QTs occur with a change in the fermion parity. For the chain with the open boundaries, the aforementioned cascade of quantum transitions occurs with the change in P, near which the MCE anomalies manifest themselves (solid lines in Fig. 3). Thus, the MCE anomalies can serve as a tool for revealing the parameters at which in the case of short open nanowires QTs occur with a change in the fermion parity of the ground state, whereas topological transitions occur in long closed nanowires.

5. STABILITY OF THE FERMION PARITY CHANGE LINES WITH RESPECT TO WEAK COULOMB INTERACTIONS

We solve the problem concerning the structure of the nanowire ground state taking into account the onsite ($\mathcal{H}_U$) and intersite ($\mathcal{H}_V$) Coulomb interactions

$$\mathcal{H}_U = U\sum_{n=1}^{N} a_{n\uparrow}^+ a_{n\downarrow}^+ a_{n\downarrow} a_{n\uparrow}, \quad U > 0,$$
$$\mathcal{H}_V = V\sum_{n=1,\sigma,\sigma'}^{N-1} a_{n\sigma}^+ a_{n+1\sigma'}^+ a_{n+1\sigma'} a_{n\sigma}, \quad V > 0 \quad (11)$$

using two methods.

Within the first approach, we employ the exact diagonalization of the Hamiltonian describing the

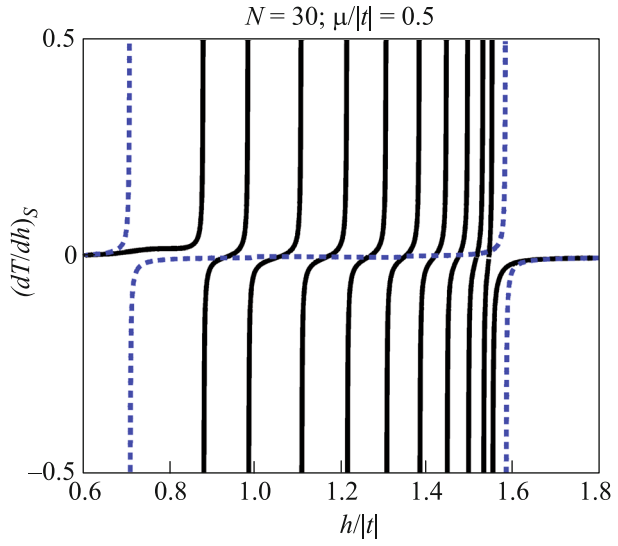

Fig. 3. (Color online) Magnetic field dependence of the magnetocaloric effect for the chain consisting of 30 sites. Here, $T = 10^{-3}|t|$ and the other parameters are the same as in Fig. 2. The comparison to Fig. 1 shows that the MCE magnitude is characterized by an anomalous behavior near quantum transitions with the change in the fermion parity of the nanowire ground state.

chain containing a small number of sites. Then, on the basis of the Lehmann representation [31]

$$-i\langle T_t \tilde{a}^+_{n\sigma}(t)\tilde{a}^+_{n'\sigma'}(t')\rangle_\omega = \sum_{s=1}^{4^N}\left(\frac{\left(a^+_{n\sigma}\right)_{0s}\left(a_{n'\sigma'}\right)_{s0}}{\omega - E_s + E_0 + i\delta} + \frac{\left(a_{n'\sigma'}\right)_{0s}\left(a^+_{n\sigma}\right)_{s0}}{\omega + E_s - E_0 - i\delta}\right), \quad (12)$$

we find the Fermi excitation energies and determine their minimum values. These exact results are used to test the accuracy of the approximate approach allowing us to calculate the characteristics of the nanowire having a large number of sites.

The second approach corresponds to the generalized mean-field approximation. Its technical aspects are related to the application of the Bogoliubov transformation to the four-fermion operators with the consequent renormalization of the operator terms [32, 33]. In such an approach, the equations for the transformation coefficients become nonlinear since the effective quadratic form of the Hamiltonian becomes dependent on the transformation parameters.

In our case, the renormalization of the matrices introduced above can be represented in the form ($A_{\sigma\sigma} = A^+_{\sigma\sigma}$; $B_{\sigma\sigma} = -B^T_{\sigma\sigma}$)

$$\left(A_{\sigma\sigma}\right)_{n,n} = -\mu + \sigma h + U\langle a^+_{n,\bar{\sigma}}a_{n,\bar{\sigma}}\rangle + V\left(\sum_{\sigma'}\langle a^+_{n-1,\sigma'}a_{n-1,\sigma'}\rangle + \langle a^+_{n+1,\sigma'}a_{n+1,\sigma'}\rangle\right),$$

$$\left(A_{\sigma\sigma}\right)_{n+1,n} = -\frac{t}{2} - V\langle a^+_{n\sigma}a_{n+1,\sigma}\rangle,$$

$$\left(A_{\uparrow\downarrow}\right)_{n,n} = -U\langle a^+_{n\downarrow}a_{n\uparrow}\rangle,$$

$$\left(A_{\uparrow\downarrow}\right)_{n,n+1} = -\frac{\alpha}{2} - V\langle a^+_{n+1\downarrow}a_{n\uparrow}\rangle,$$

$$\left(A_{\uparrow\downarrow}\right)_{n+1,n} = \frac{\alpha}{2} - V\langle a^+_{n\downarrow}a_{n+1\uparrow}\rangle,$$

$$\left(B_{\sigma\sigma}\right)_{n+1,n} = -V\langle a_{n+1\sigma}a_{n\sigma}\rangle,$$

$$\left(B_{\uparrow\downarrow}\right)_{n,n} = -\Delta^* + U\langle a_{n\downarrow}a_{n\uparrow}\rangle,$$

$$\left(B_{\uparrow\downarrow}\right)_{n,n+1} = V\langle a_{n+1\downarrow}a_{n\uparrow}\rangle,$$

$$\left(B_{\uparrow\downarrow}\right)_{n+1,n} = -V\langle a_{n+1\uparrow}a_{n\downarrow}\rangle. \quad (13)$$

The averages in these expressions are nonlinearly related to the sought parameters of the Bogoliubov transformation

$$\langle a^+_{n\sigma}a_{n'\sigma'}\rangle = \sum_{m=1}^{2N}\left[u_{n\sigma,m}u^*_{n'\sigma',m}f\left(\frac{\varepsilon_m}{T}\right) + v_{n\sigma,m}v^*_{n'\sigma',m}\left(1 - f\left(\frac{\varepsilon_m}{T}\right)\right)\right], \quad (14)$$

$$\langle a^+_{n\sigma}a^+_{n'\sigma'}\rangle = \sum_{m=1}^{2N}\left[u_{n\sigma,m}v_{n'\sigma',m}f\left(\frac{\varepsilon_m}{T}\right) + v_{n\sigma,m}u_{n'\sigma',m}\left(1 - f\left(\frac{\varepsilon_m}{T}\right)\right)\right], \quad (15)$$

where $f(x)$ is the Fermi–Dirac function. This approach provides an algorithm where the transformation coefficients are determined from the solution to the self-consistent set of nonlinear equations.

For short chains ($N = 6$), the comparison of the results obtained by the two described calculation techniques demonstrates that, at $U, V \lesssim |t|$, the low-energy branches of the excitation spectrum ε_m and the one-particle wavefunctions corresponding to them coincide within an accuracy of several percent. Accordingly, the parametric lines exhibiting the change in the fermion parity of the ground state are also well reproduced in the mean-field approach. All these statements are illustrated in Fig. 4 for the case of $U = 0.5|t|$ and $V = 0.3|t|$.

The spectral characteristics and features of the ground state for nanowires with a large number of sites taking into account the Coulomb interactions were calculated in the generalized mean-field approximation. It turns out that the aforementioned features of the systems remain unchanged even in the presence of electron–electron interactions: for infinite closed chains, there exists a parameter range where the topologically nontrivial phase appears. When the parame-

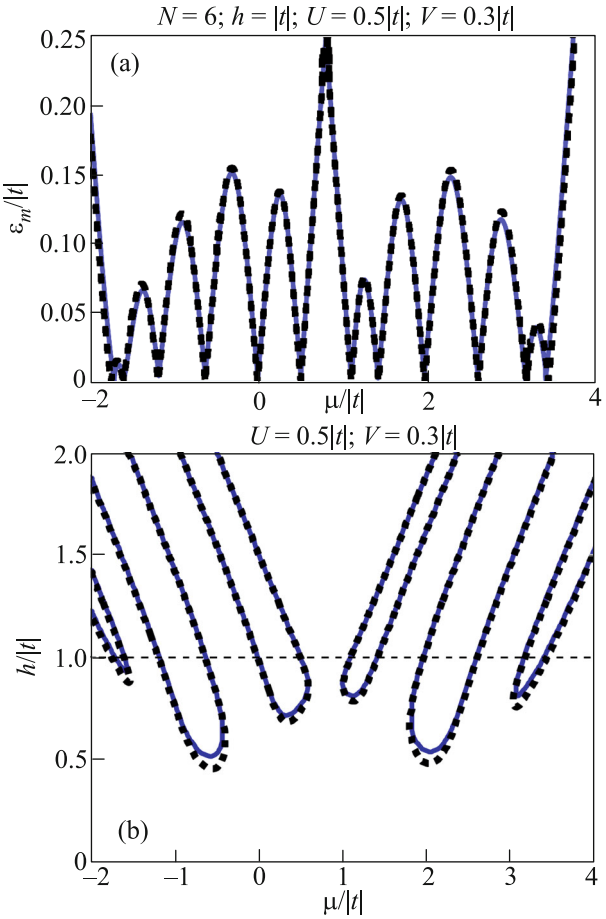

Fig. 4. (Color online) (a) Minimum excitation energy for the open nanowire with the Coulomb interactions at $N = 6$, $h = |t|$, $U = 0.5|t|$, and $V = 0.3|t|$ versus the chemical potential (upper panel). The solid curve corresponds to the energy calculated in the generalized mean-field approximation. The dashed line corresponds to the energy calculated by the exact diagonalization and the Lehmann representation. (b) Boundaries of the phases (at the same values of parameters) with the negative fermion parity for the nanowire obtained with allowance for Coulomb interactions. Solid lines correspond to the generalized mean-field approximation and the dashed curves show the results of exact calculations. The other parameters not mentioned here are the same as in Fig. 1.

ters are varied within this range, a cascade of QTs occurs in an open short chain with the change in the fermion parity of the ground state, which is accompanied by the magnetocaloric anomalies.

Figure 5 shows the fermion parity map for the open short chain and topological transition lines for the closed long chain in the case of $U = 0.5|t|$, $V = 0.3|t|$, and the other parameters corresponding to Fig. 1. We can see that QTs are retained even in the presence of electron correlations, whereas the lines of quantum critical points change their location in the phase diagram.

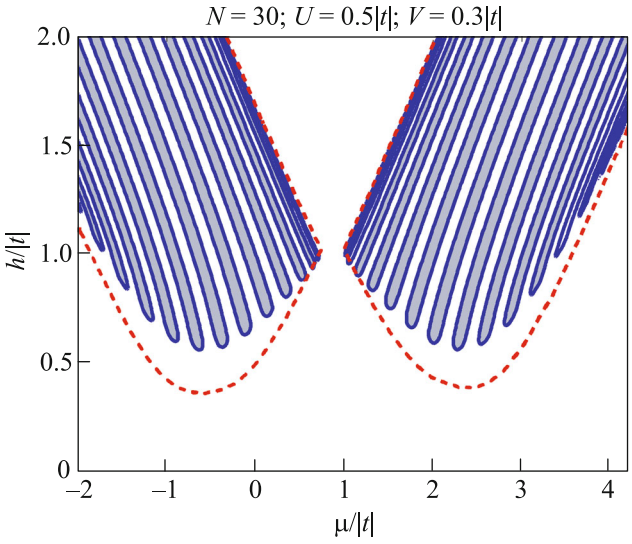

Fig. 5. (Color online) Map of the fermion parity for the open chain consisting of 30 sites and the boundaries of the topological phases (dashed lines) for the closed infinitely long chain obtained with allowance for electron correlations: $U = 0.5|t|$, $V = 0.3|t|$. The other parameters are the same as in Fig. 1. At the parameters corresponding to the shaded areas, the ground state of the open chain includes the partial contributions corresponding to odd numbers of fermions.

6. CONCLUSIONS

The main result of this work is the prediction of the anomalous behavior of the magnetocaloric effect in open short ($L \sim 10-100$ nm) semiconductor nanowires with the strong Rashba spin–orbit coupling and the induced superconducting pairing potential. Such behavior arises within the magnetic field range where the topological index for the closed infinite nanowire (the Majorana number) is negative and the state of this nanowire corresponds to the topologically nontrivial phase.

The anomalous behavior occurs because, for an open nanowire with a finite number of sites, the parameter range where the state of the infinite nanowire is topologically nontrivial becomes separated into a finite number of subranges; within each of them, the fermion parity of the ground state is negative. The boundaries of such subranges are the lines consisting of points corresponding to the doubly degenerate ground state and having excitations including the zeroth mode. The crossing of each boundary is accompanied by the quantum transition with the change in the fermion parity of the ground state.

It is important that the aforementioned quantum transition is accompanied by the change in the sign of the magnetocaloric effect, whereas the magnitude of the magnetocaloric effect at the quantum critical point tends to infinity. Such a scenario is repeated at each crossing of the quantum critical point. This

explains the origin of the cascade of quantum transitions occurring in a finite nanowire with the change in the applied magnetic field.

It is shown that the cascade of quantum transitions takes place even in the presence of the electron–electron interactions in the nanowire. The positions of the corresponding quantum critical points on the phase diagram can also be found by analyzing the magnetocaloric anomalies.

An important practical aspect of the predicted cascade of quantum transitions is that the parameter range corresponding to the topologically nontrivial phase for the closed infinite nanowire with the strong Rashba spin–orbit coupling and the induced superconducting pairing potential can be identified by analyzing the specific features characterizing the behavior of the magnetocaloric effect in an open short nanowire.

We are grateful to A.D. Fedoseev and A.O. Zlotnikov for the useful comments and discussions of the results. This work was supported jointly by the Russian Foundation for Basic Research, the Government of the Krasnoyarsk Territory, and the Krasnoyarsk Territorial Foundation for the Support of R&D Activities (project nos. 16-42-243056r, 16-42-243057, and 17-42-240441), as well as by the Russian Foundation for Basic Research (project no. 16-02-00073).

REFERENCES

1. A. Y. Kitaev, Phys. Usp. **44**, 131 (2001).
2. M. Sato and S. Fujimoto, J. Phys. Soc. J. **85**, 072001 (2016).
3. E. M. Stoudenmire, J. Alicea, O. A. Starykh, and M. P. A. Fisher, Phys. Rev. B **84**, 014503 (2011).
4. T.-P. Choy, J. M. Edge, A. R. Akhmerov, and C. W. J. Beenakker, Phys. Rev. B **84**, 195442 (2011).
5. Y.-M. Lu and Z. Wang, Phys. Rev. Lett. **110**, 096403 (2013).
6. J. Li, H. Chen, I. K. Drozdov, A. Yazdani, B. A. Bernevig, and A. H. MacDonald, Phys. Rev. B **90**, 235433 (2014).
7. G. E. Volovik, JETP Lett. **90**, 398 (2009).
8. M. A. Silaev and G. E. Volovik, J. Exp. Theor. Phys. **119**, 1042 (2014).
9. A. Yu. Kitaev, Ann. Phys. **321**, 2 (2006).
10. V. V. Val'kov, A. O. Zlotnikov, A. D. Fedoseev, and M. S. Shustin, J. Magn. Magn. Mater. **440**, 37 (2017).
11. A. P. Schnyder, S. Ryu, A. Furusaki, and A. W. W. Ludwig, Phys. Rev. B **78**, 195125 (2008).
12. A. Yu. Kitaev, AIP Conf. Proc. **1134**, 22 (2009).
13. A. M. Turner, F. Pollmann, and E. Berg, Phys. Rev. B **83**, 075102 (2011).
14. L. Fidkowski and A. Yu. Kitaev, Phys. Rev. B **83**, 075103 (2011).
15. E. M. Stoudenmire, J. Alicea, O. A. Starykh, and M. P. A. Fisher, Phys. Rev. B **84**, 014503 (2011).
16. M. Guigou, N. Sedlmayr, J. M. Aguiar-Hualde, and C. Bena, Eur. Phys. Lett. **115**, 47005 (2016).
17. P. Szumniak, D. Chevallier, D. Loss, and J. Klenovaja, Phys. Rev. B **96,** 041401(R) (2017).
18. V. Mourik, K. Zuo, S. M. Frolov, S. R. Plissard, E. Bakkers, and L. P. Kouwenhoven, Science **336**, 1003 (2012).
19. A. Das, Y. Ronen, Y. Most, Y. Oreg, M. Heiblum, and H. Shtrikman, Nat. Phys. **8**, 887 (2012).
20. S. Nadj-Perge, I. K. Drozdov, J. Li, H. Chen, S. Jeon, Ju. Seo, A. H. MacDonald, B. A. Bernevig, and A. Yazdani, Science **346**, 602 (2014).
21. F. Pientka, G. Kells, A. Romito, P. W. Brouwer, and F. von Oppen, Phys. Rev. Lett. **109**, 227006 (2012).
22. J. Liu, A. C. Potter, K. T. Law, and P. A. Lee, Phys. Rev. Lett. **109**, 267002 (2012).
23. N. Sedlmayr and C. Bena, Phys. Rev. B **92**, 115115 (2015).
24. N. Sedlmayr, J. M. Aguiar-Hualde, and C. Bena, Phys. Rev. B **93**, 155425 (2016).
25. O. Dmytruk and J. Klenovaja, arXiv:1710.01671v1 (2017).
26. F. Pientka, A. Romito, M. Duckheim, Y. Oreg, and F. von Oppen, New J. Phys. **15**, 025001 (2013).
27. A. A. Zvyagin, Low Temp. Phys. **41**, 806 (2015).
28. S. Hegde and S. Vishveshwara, Phys. Rev. B **94**, 115166 (2016).
29. L. Zhu, M. Garst, A. Rosch, and Q. Si, Phys. Rev. Lett. **91**, 066404 (2003).
30. M. Garst and A. Rosch, Phys. Rev. B **72**, 205129 (2005).
31. H. Lehmann, Nuovo Cimento **11**, 342 (1954).
32. B. G. Kukharenko, Sov. Phys. JETP **42**, 321 (1975).
33. V. V. Val'kov and T. A. Val'kova, Sov. Phys. JETP **72**, 1053 (1991).

Translated by K. Kugel